FEBS Letters 541 (2003) 126–131 FEBS 27166

In situ observation of mobility and anchoring of PKCβI in plasma membrane

Kenta Saito[a], Eiko Ito[b], Yuichi Takakuwa[b], Mamoru Tamura[a], Masataka Kinjo[a,*]

[a] *Laboratory of Supramolecular Biophysics, Research Institute for Electronic Science, Hokkaido University, N12W6, Kita-ku, Sapporo 060-0812, Japan*
[b] *Department of Biochemistry, School of Medicine, Tokyo Women's Medical College, Shinjuku, Tokyo 162-8666, Japan*

Received 8 January 2003; revised 18 March 2003; accepted 25 March 2003

First published online 3 April 2003

Edited by Michael R. Bubb

Abstract We employed fluorescence correlation spectroscopy (FCS) to analyze the characteristics of biomolecules in living cells. Protein kinase C (PKC) changes its subcellular localization from cytosol to the plasma membrane by its ligand. Using FCS, we found PKCβI labeled with enhanced green fluorescent protein freely diffusing in cytosol. Upon 12-*O*-tetradecanoylphorbol-13-acetate activation, a large part of PKCβI is anchored in the plasma membrane but some PKCβI still moves freely near the plasma membrane. These results indicate that a diffusion-driven transport mechanism is appropriate for the molecular mechanism of the PKCβI localization change.

Key words: Fluorescence correlation spectroscopy; Protein kinase C; Green fluorescent protein; Diffusion constant; Signal transduction; Plasma membrane

1. Introduction

Fluorescence correlation spectroscopy (FCS) is one of the techniques used to assess protein interactions in aqueous conditions at the single-molecule level [1]. FCS measures the fluctuations in fluorescence intensity caused by fluorescent probe movement in a small light cavity with a defined volume (0.25 fl) generated by confocal illumination. The average residence time (τ) and the absolute number of probes in the small volume can be deduced by the fluorescence autocorrelation function (FAF) calculated from measured fluctuations. FCS has been used to inquire into the molecular kinetics of biophysical and biochemical reactions in vitro [2–6]. FCS can also measure the kinetics of reactions and analysis of microenvironment inside a single living cell [7–13].

Protein kinase C (PKC) is recognized as one of the key enzymes in signal transduction and is related to the control of many aspects of cellular function [14]. PKCβI, one of the subtypes of conventional PKC, undergoes a localization change from cytosol to the plasma membrane upon activation by various intracellular signaling factors such as diacylglycerol or phorbol ester (e.g. 12-*O*-tetradecanoylphorbol-13-acetate (TPA)) [15,16]. Recent observations of PKC fused with green fluorescent protein (GFP) under confocal scanning fluorescence microscopy in living cells have clearly revealed the subcellular localization of each PKC subtype [17–19].

However, it is still unclear (i) whether PKCβI is free or bound to another protein in cytosol before stimulation, (ii) how PKCβI is fixed on the surface of the plasma membrane after the localization change, and (iii) how PKCβI moves from cytosol to the membrane and whether PKCβI needs another protein for the localization change. These subjects have not been studied using classical biological techniques. By using FCS, we examined these aspects of PKCβI.

2. Materials and methods

2.1. Cell culture and transfection with plasmid DNA

Human embryonic kidney 293 (HEK293) cells were grown in a 5% CO_2 humidified atmosphere at 37°C in Dulbecco's modified Eagle's medium (DMEM) supplemented with 10% fetal bovine serum, 2×10^5 U/l penicillin G, and 200 mg/l streptomycin sulfate. Cells were propagated every 1 or 2 days. For transient expression, cells were plated at a confluence of 10–20% on LAB-TEK chambered coverslips with eight wells (Nalge Nunc International, Naperville, IL, USA) for 12 h before transfection. DMEM (20 μl) and FuGENE 6 (1.2 μl, Roche Molecular Biochemicals, Mannheim, Germany) were mixed. Five minutes after mixing, 0.4 μg of the EGFP-C1 or PKCβI-EGFP coding plasmid DNA (Clontech, Palo Alto, CA, USA) was added to the prediluted FuGENE 6 solution. The DNA solution was left for 15 min and added to one well at 12 h before FCS measurement.

2.2. Microscopy

Live cell fluorescence microscopy was performed using an LSM510 inverted confocal laser scanning microscope (LSM, Carl Zeiss, Jena, Germany). EGFP was excited at the 488 nm laser line of a CW Ar^+ laser through a water immersion objective (C-Apochromat, 40×, 1.2 NA; Carl Zeiss) with emission detected at >505 nm. Pinhole diameter was adjusted to 70 μm.

2.3. FCS setup

FCS measurements were carried out with a ConfoCor and ConfoCor2 (Carl Zeiss) that consisted of a CW Ar^+ laser, a water immersion objective (C-Apochromat, 40×, 1.2 NA; Carl Zeiss), an avalanche photodiode (SPCM-200-PQ, EG&G, Quebec, QC, Canada) and a digital correlator (ALV 5000/E, ALV, Langen, Germany) for the ConfoCor. Confocal pinhole diameter was adjusted to 30 μm and 70 μm for the ConfoCor and ConfoCor2, respectively. Samples were excited with about 10 kW/cm^2 of laser power at 488 nm and the fluorescence signal was detected through a dichroic mirror (>510 nm) and a band pass filter (515–560 nm).

2.4. FCS measurement and analysis

Cells were washed with phenol red-free Hanks' balanced salt solution (HBSS) two times to remove phenol red dye, then medium was

*Corresponding author. Fax: (81)-11-706 4964.
E-mail address: kinjo@imd.es.hokudai.ac.jp (M. Kinjo).

Abbreviations: FCS, fluorescence correlation spectroscopy; FAF, fluorescence autocorrelation function; EGFP, enhanced green fluorescent protein; PKC, protein kinase C; DMEM, Dulbecco's modified Eagle's medium; HBSS, Hanks' balanced salt solution; LSM, laser scanning microscope; Rh6G, rhodamine 6G; TPA, 12-*O*-tetradecanoylphorbol-13-acetate

0014-5793/03/$22.00
doi:10.1016/S0014-5793(03)00324-7

replaced by HBSS. Immediately thereafter, FCS measurements were carried out. PKCβI activation was done by addition of 30 ng/ml TPA solution to the medium. FAFs, $G(\tau)$, were acquired online with a digital correlator and fitted with the FCS Access Fit program (EVOTEC BioSystems, Hamburg, Germany) by a one-, two-, or three-component model as follows:

$$G(\tau) = \frac{\langle I(t)I(t+\tau)\rangle}{\langle I(t)\rangle^2} = 1 + \frac{1}{N}\sum_i F_i\left(1+\frac{\tau}{\tau_i}\right)^{-1}\left(1+\frac{\tau}{s^2\tau_i}\right)^{-1/2} \quad (1)$$

where F_i and τ_i are the fraction and diffusion time of component i, respectively, N is the number of fluorescent molecules in the detection volume element defined by radius w_0 and length $2z_0$, s is the structure parameter representing the ratio, $s = z_0/w_0$. FAFs of rhodamine 6G (Rh6G) solution were measured for 60 s five times at 10-s intervals, then the diffusion time (τ_{Rh6G}) and s were obtained by one-component fitting of the measured FAFs. Diffusion constants of samples (D_{sample}) were calculated from the ratio with the diffusion constant of Rh6G D_{Rh6G} (2.8×10^{-6} cm^2/s) and diffusion times τ_{Rh6G} and τ_{sample} were obtained as the following equation:

$$\frac{D_{sample}}{D_{Rh6G}} = \frac{\tau_{Rh6G}}{\tau_{sample}} \quad (2)$$

3. Results

3.1. PKCβI-EGFP localization changes upon TPA activation

To observe the localization of EGFP and PKCβI-EGFP in HEK293 cells, confocal LSM images of HEK293 cells were taken and the fluorescence intensity of the confocal volume element according to the optical axis (z-scan) was measured. Images of HEK293 cells expressing EGFP and PKCβI-EGFP are shown in Fig. 1A. EGFP was widely distributed through the cytosol and nucleus. Even 10 min after TPA addition, the localization of EGFP was not changed. On the other hand, PKCβI-EGFP was mainly located in the cytosol but was also found in the plasma membrane. However, 10 min after TPA addition PKCβI-EGFP was mainly located in the plasma membrane.

The time course of fluorescence intensity distribution along the optical axis (z-scan) in transfected HEK293 cells is shown in Fig. 1B. In a control experiment the fluorescence intensity of EGFP was not changed even after TPA addition. Initially, that of PKCβI-EGFP was distributed through the cytosol. After TPA addition, the fluorescence intensity profile had two peaks at both sides of the membrane. From them, we could choose the measuring position of the cytosol and plasma membrane using the 2D image of LSM and also the optical axis scan (z-scan) of FCS (Fig. 1C).

3.2. FCS measurements for EGFP in living cells and in TE buffer

We measured FAFs of EGFP in living cells. Example FAFs are shown in Fig. 2. FCS measurements were carried out from the plasma membrane to cytosol in about 1-μm steps (Fig. 2A). In the plasma membrane region, since the plasma membrane is very thin (~4 nm), the confocal volume contains both cytosol and membrane, where fast and slow components may coexist. However, similar correlation curves were also obtained at positions 1 (membrane) to 4 (cytosol) (Fig. 2C). Because EGFP does not interact with plasma membrane, there was no contribution from interaction with the plasma membrane. Therefore, most of the fraction was free-moving molecules, which were observed even at position 1.

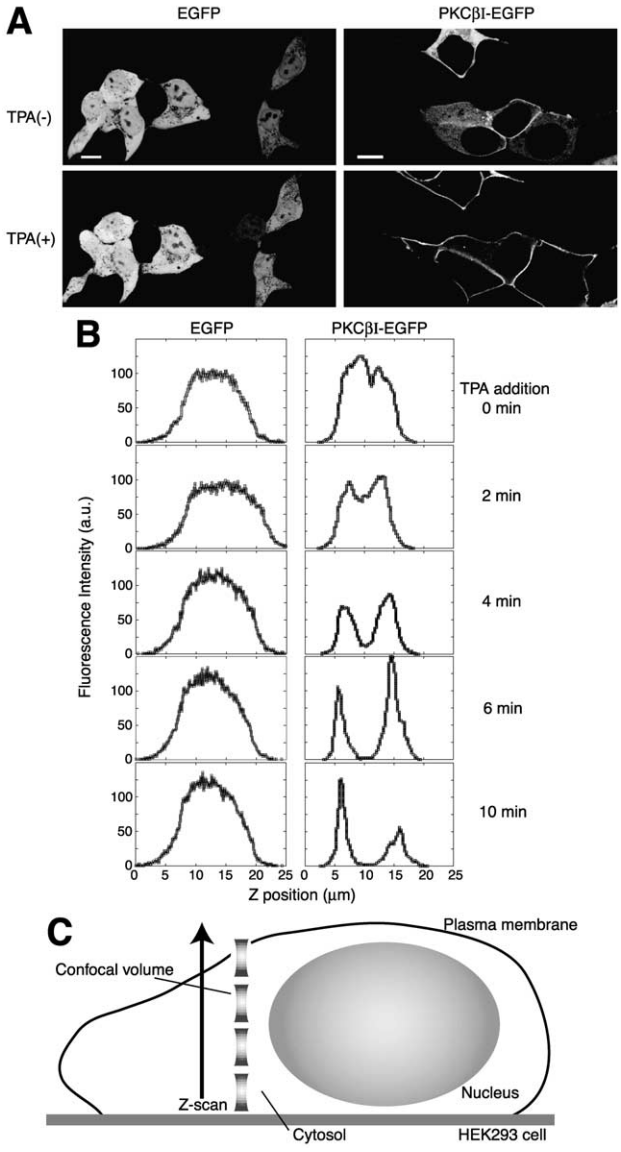

Fig. 1. Localization and translocation of PKCβI-EGFP. A: Transfected HEK293 cells with EGFP (left) and PKCβI-EGFP (right) were imaged using a confocal LSM before (upper) and 10 min after (lower) TPA addition. Scale bars represent 10 μm. B: The z-scan time course through transfected HEK293 cells was observed after TPA addition. C: The z-scan was performed using an FCS system.

All FAFs for in vitro measurements could be fitted to one component. See, for example, TE measurement in Fig. 2C. However, for in vivo measurements, the number of components was not pre-fixed since the state of the target molecules in living cells was unknown. Thus in vivo measurements could be fitted not only to one component but to two or three components according to the flow chart of the evaluation procedure reported previously [12]. We also analyzed fluorescence autocorrelation functions in a model that included 2D and 3D components. The parameters (diffusion constant and fraction) obtained from this analysis were not so different from those in the analysis in the model that included 3D components only. Therefore in this study, we used the model that included 3D components only. The averages of the diffusion constants and fractions of EGFP in the cytosol and in the plasma membrane region are shown in Table 1. More

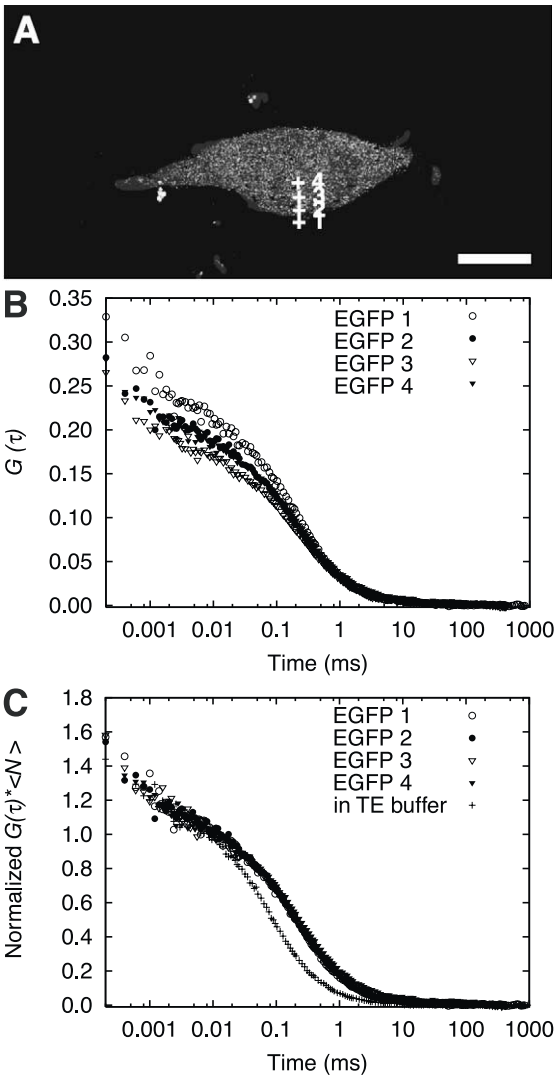

Fig. 2. Diffusion of EGFP. A: EGFP-transfected HEK293 cell and measurement positions. Scale bar represents 10 μm. B: FAF of EGFP at the measurement positions from the plasma membrane to cytosol in about 1-μm steps. Numbers of measurement positions shown in A correspond to numbers in B. C: Normalized FAF of B and that in TE buffer.

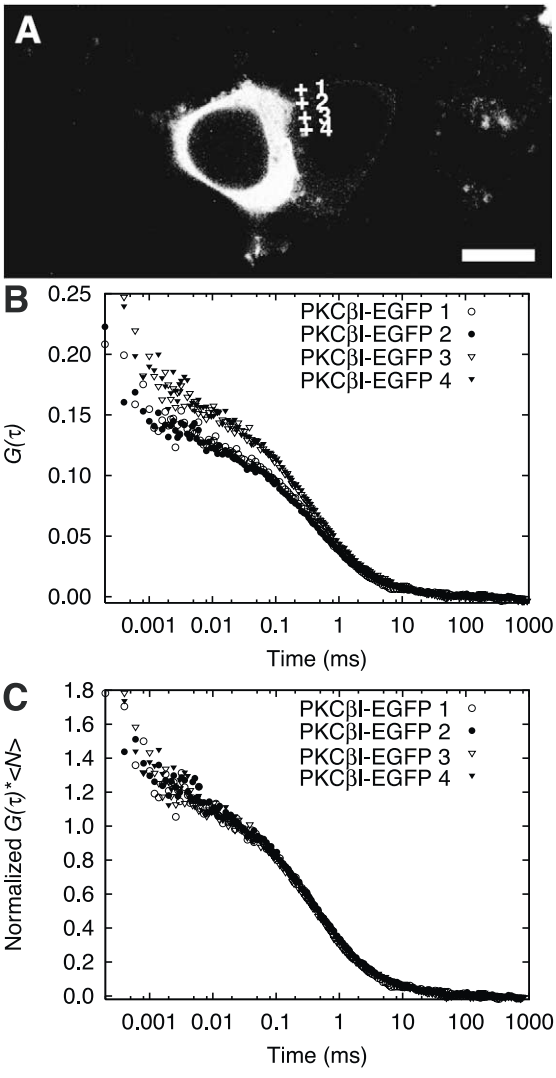

Fig. 3. Diffusion of PKCβI-EGFP. A: PKCβI-EGFP-transfected HEK293 cell and measurement positions. Scale bar represents 10 μm. B: FAF of PKCβI-EGFP at the measurement positions from the plasma membrane to cytosol in about 1-μm steps. Numbers of measurement positions shown in A correspond to numbers in B. C: Normalized FAF of B.

than 95% of the fraction of EGFP in the cytosol was defined as the first component, which means free diffusion. These results were highly reproducible and independent within the cytosol position. The first components are presumed to represent the freely diffusing EGFP in cytosol. The second components are considered to represent the slowly diffusing EGFP. The high density of the cellular solute may prevent free, rapid diffusion of EGFP. The third components might represent the

Table 1
Difference between subcellular location and effect of TPA addition on the diffusion of EGFP

		First		Second		Third	
	n	D_1 (cm^2/s)	F_1 (%)	D_2 (cm^2/s)	F_2 (%)	D_3 (cm^2/s)	F_3 (%)
Cytosol							
TPA(−)	133	$2.5\pm1.0\times10^{-7}$*†	98.6	$9.1\pm9.4\times10^{-9}$	1.4	–	–
TPA(+)	85	$2.4\pm0.8\times10^{-7}$	97.5	$1.0\pm1.3\times10^{-8}$	2.4	2.8×10^{-9}	0.1
Membrane							
TPA(−)	90	$2.4\pm1.1\times10^{-7}$	96.2	$9.4\pm8.8\times10^{-9}$	3.6	2.9×10^{-11}	0.2
TPA(+)	77	$2.5\pm1.2\times10^{-7}$	92.9	$1.2\pm1.2\times10^{-8}$	6.8	3.8×10^{-11}	0.2
TE buffer	13	$8.9\pm0.5\times10^{-7}$*	100	–	–	–	–

The diffusion constants (D), fraction (F) and number (n) of FCS measurements for EGFP in cytosol and in the plasma membrane region in the absence (TPA(−)) and presence (TPA(+)) of TPA and of EGFP in TE buffer.
*Significantly different ($P<0.001$). †Significantly different ($P<0.001$) between Tables 1 and 2.

apparent diffusion caused by a fluorescence intensity decrease. There was no significant difference between the average D_1 of EGFP in cytosol and that in the plasma membrane region, as the membrane contribution to mobility was very small even in the plasma membrane region, as shown in Fig. 2B,C. Nor was there any significant difference between the average D_1 of EGFP in the absence and presence of TPA. D_1 of EGFP in cytosol was about three times smaller than that in TE buffer. This result indicates that the viscosity of the cytosol was only about three times that in TE buffer.

3.3. FCS measurements for PKCβI-EGFP in living cells

We also measured FAFs of PKCβI-EGFP in living cells. In the FCS measurement, we targeted not brightly fluorescent cells but weakly fluorescent ones because FCS has a high sensitivity. For example, the cell on the left in Fig. 3A was not suitable for FCS measurement, so we carried out FCS measurement in the cell on the right. Typical FAFs are shown in Fig. 3. FCS measurements were carried out from the plasma membrane to cytosol in about 1-μm steps (Fig. 3A). There were no significant differences between the FAF of PKCβI-EGFP at positions from the plasma membrane to cytosol in the absence of TPA (Fig. 3B,C). However, after TPA addition to the same cell (Fig. 4A), the amplitude of FAF increased from the plasma membrane to the cytosol, which meant a decrease of the mean number $\langle N \rangle$ of PKCβI-EGFP molecules from the plasma membrane to cytosol, which agreed with the translocation of the protein (Fig. 4B). In the plasma membrane region (position 1), FAF differed from those of the others, a typical multicomponent function (Fig. 4C). On the other hand, positions 2–4 were similar to the FAFs before TPA addition.

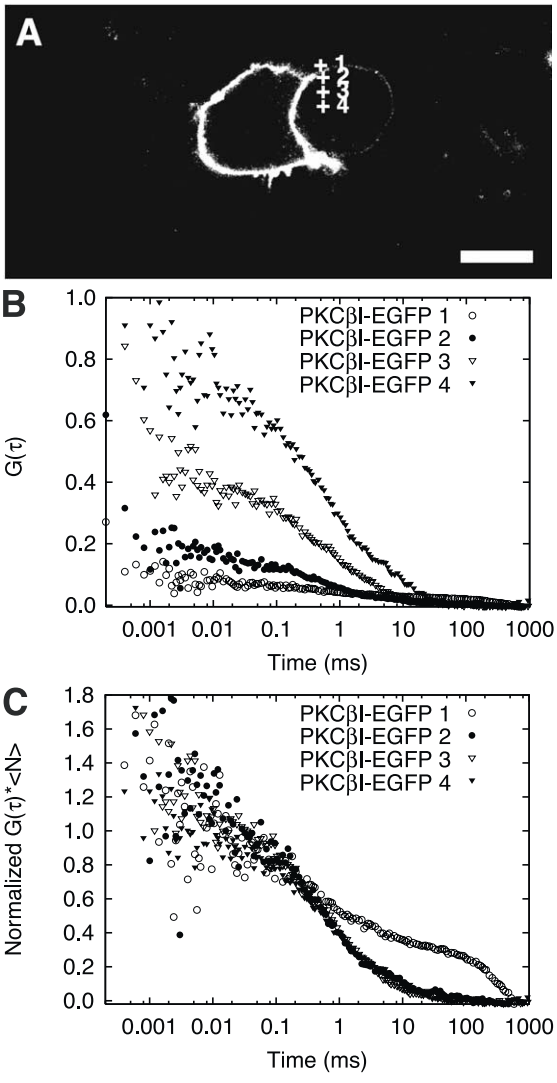

Fig. 4. Diffusion of PKCβI-EGFP after TPA addition. A: PKCβI-EGFP-transfected HEK293 cell after TPA addition and measurement positions. B: FAF of PKCβI-EGFP at the measurement positions from the plasma membrane to cytosol in about 1-μm steps. Numbers of measurement positions shown in A correspond to numbers in B. C: Normalized FAF of B. Mean numbers $\langle N \rangle$ of PKCβI-EGFP molecules obtained from FAFs were 12.7, 7.1, 2.8 and 1.4 at positions 1–4, respectively.

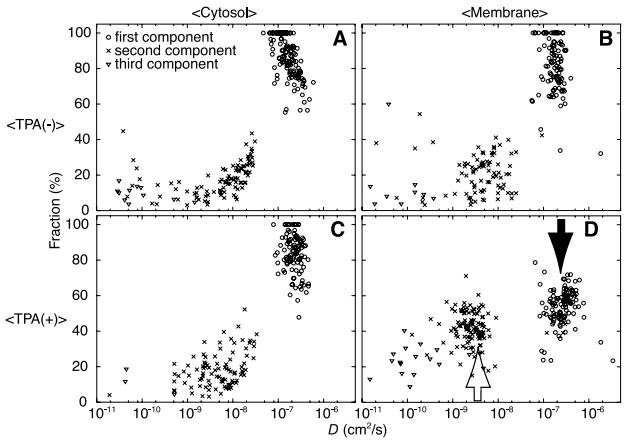

Fig. 5. Statistical analysis of diffusion constants. Dispersion plots of diffusion constants and their fractions from FCS measurements for PKCβI-EGFP in cytosol and in the plasma membrane region in the absence (TPA(−)) and presence (TPA(+)) of TPA. First, second and third components are shown with different symbols.

Fig. 5 shows the dispersion plots of D and the fraction from FCS measurements of PKCβI-EGFP. All obtained plots were distributed mainly into two clusters. The first components were grouped into one cluster between 10^{-7} and 10^{-6} cm^2/s and presumed to represent the free diffusion of PKCβI-EGFP in cytosol. The second components were between 10^{-11} and 5×10^{-8} cm^2/s and considered to represent the slow diffusion of PKCβI-EGFP that interacted with inner cellular components and the plasma membrane. Actually, we cannot detect immobile complexes by using FCS, but we can estimate the fraction of the immobile component from the degree of photobleaching during FCS measurement. However, a detailed discussion and studies about photobleaching in FCS measurement are beyond the focus of this paper. In the absence of TPA, the distributions of D in cytosol and in the plasma membrane were similar. However, in the presence of TPA, at the plasma membrane region the plots of the clusters between 10^{-11} and 5×10^{-8} cm^2/s shifted to an increase (Fig. 5D, white arrow), and the number of plots of the cluster between 10^{-7} and 10^{-6} cm^2/s decreased (Fig. 5D, dark arrow).

The averages of the diffusion constants and fractions of PKCβI-EGFP in the cytosol and that in the plasma membrane region are shown in Table 2. The D_1 values of non-

Table 2
Difference between subcellular location and effect of TPA addition on the diffusion of PKCβI-EGFP

		First		Second		Third	
	n	D_1 (cm^2/s)	F_1 (%)	D_2 (cm^2/s)	F_2 (%)	D_3 (cm^2/s)	F_3 (%)
Cytosol							
TPA(−)	132	$1.8 \pm 0.9 \times 10^{-7\dagger}$	86.2	$1.0 \pm 0.9 \times 10^{-8}$	12.7	$1.9 \pm 4.0 \times 10^{-10}$	1.1
TPA(+)	110	$2.4 \pm 0.8 \times 10^{-7}$	84.2	$7.7 \pm 7.5 \times 10^{-9}$	15.5	$2.0 \pm 2.7 \times 10^{-10}$	0.3
Membrane							
TPA(−)	103	$2.0 \pm 1.7 \times 10^{-7}$	81.7	$7.6 \pm 11 \times 10^{-9}$	16.7*	$5.5 \pm 14 \times 10^{-10}$	1.5
TPA(+)	115	$4.1 \pm 10 \times 10^{-7}$	53.9	$8.7 \pm 39 \times 10^{-9}$	42.1*	$9.2 \pm 16 \times 10^{-10}$	4.0

Diffusion constants (D), fraction (F) and number (n) of FCS measurements for PKCβI-EGFP in cytosol and in the plasma membrane region in the absence (TPA(−)) and presence (TPA(+)) of TPA. *Significantly different ($P < 0.001$). †Significantly different ($P < 0.001$) between Tables 1 and 2.

activated PKCβI-EGFP in cytosol and in the plasma membrane region were similar to each other and were about 1.4 times slower than that of EGFP. This D_1 ratio agreed with the predicted value calculated from the cube root of EGFP and the PKCβI-EGFP molecular weight ratio, according to the Stokes–Einstein equation. F_1 and F_2 in the plasma membrane were changed after TPA addition. The F_1 in the plasma membrane became 53.9% and the F_2 in the plasma membrane region became 42.1% (Table 2). A possible explanation for the larger changes in D_1 in cytosol in the presence of TPA is an apparent increase of D caused by a decrease of fluorescence intensity. We could not measure the precise diffusion constant on PKCβI-EGFP in cytosol in the presence of TPA because of the low fluorescence intensity and low S/N ratio.

4. Discussion

We applied fluorescence correlation spectroscopy to measure the diffusion of PKCβI in the living cell. First, we observed the diffusion of PKCβI in cytosol in the inactive state. The measured D_1 agreed with the predicted value calculated from the cube root of EGFP and the PKCβI-EGFP molecular weight ratio, according to the Stokes–Einstein equation. Thus, like EGFP, PKCβI in the inactive state was not bound with other proteins or macromolecules in cytosol or near the plasma membrane.

Second, we measured the diffusion of PKCβI after the localization change. As seen in Figs. 4 and 5, a significant amount of translocated PKCβI near the plasma membrane still moved freely. There might have been reversible binding of PKCβI to the plasma membrane surface in the presence of TPA. Our results directly confirm the model for PKCβI translocation previously proposed [20] with respect to the weak interaction in unstimulated cells between PKCβI and an anchoring component (Fig. 5B, Table 2). After PKCβI translocated to the plasma membrane, the fraction of slow movement (second component) that interacted with the plasma membrane increased from 16.7% to 42.1% (Fig. 5D, Table 2). Thus, there might have been lateral diffusion of membrane-bound PKCβI. Some reports have suggested that PKCβI interacts primarily with the surface of the lipid membrane, and others have proposed that PKCβI binds membrane-anchoring proteins (receptor for activated C kinase or RACKs) and then phosphorylates its substrates [15,16,20]. The rather wide range of D_2 of PKCβI-EGFP at the plasma membrane in the presence of TPA (Fig. 5D) showed that PKCβI might interact with membrane lipids (TPA, phosphatidylserine) and/or RACKs. PKCβI might have been localized on the plasma membrane by reversible binding of PKCβI to the plasma membrane and/or lateral diffusion at the plasma membrane. However, further study is needed to detect the direct interaction between PKCβI and its ligand by means of dual-color fluorescence cross-correlation spectroscopy [21].

Finally, we will discuss the mechanism of the PKCβI localization change from cytosol to the plasma membrane. The PKCβI localization change does not need specific biochemical systems, such as cytoskeleton or energy-dependent motor proteins that are essential for some types of protein trafficking, for example, axonal flow and vesicle transport [17]. In human erythrocytes, which do not have a transport system, an increase of PKC activity in the plasma membrane was demonstrated [22]. Although a diffusion-driven translocation mechanism was found by confocal line-scan microscopy to follow subcellular PKC concentrations at high spatiotemporal resolution [23], this measurement still required overexpression of PKC. In contrast, FCS measurement can be carried out in diluted conditions (see Fig. 3A) so that our results represent a more native condition of PKC in the living cell. In this study we found that inactive PKCβI moved rapidly in cytosol ($D_1 = 1.8 \times 10^{-7}$ cm^2/s). Assuming a random walk by diffusion, it would take about 2.5 s to travel a distance of 10 μm, which is about the distance from the center of a cell to the plasma membrane. This calculation indicates that a diffusion-driven transport mechanism is appropriate for the molecular mechanism of the PKC localization change. Upon TPA activation, PKC freely diffuses in cytosol and often collides with TPA in the plasma membrane. PKCβI is anchored in the plasma membrane when successful binding events between PKCβI and TPA occur. Our results were obtained from only HEK293 cells. We plan to examine another cell line in order to confirm our results in a future experiment.

These aspects of PKCβI were not clarified by using classical biological techniques. Thus, FCS is a useful tool for investigating the molecular mechanism of dynamic events like the PKCβI localization change in living cells.

References

[1] Rigler, R., Mets, Ü., Widengren, J. and Kask, P. (1993) Eur. Biophys. J. 22, 169–175.
[2] Kinjo, M., Nishimura, G., Koyama, T. and Mets, Ü. (1998) Anal. Biochem. 260, 166–172.
[3] Pack, C.-G., Nishimura, G., Tamura, M., Aoki, K., Taguchi, H., Yoshida, M. and Kinjo, M. (1999) Cytometry 36, 247–253.
[4] Takakuwa, Y., Pack, C.-G., An, X.-L., Manno, S., Ito, E. and Kinjo, M. (1999) Biophys. Chem. 82, 149–155.

[5] Pack, C.-G., Aoki, K., Taguchi, H., Yoshida, M., Kinjo, M. and Tamura, M. (2000) Biochem. Biophys. Res. Commun. 267, 300–304.
[6] Bastiaens, P.I.H. and Pepperkok, R. (2000) Trends Biochem. Sci. 25, 631–637.
[7] Brock, R., Vàmosi, G., Vereb, G. and Jovin, T.M. (1999) Proc. Natl. Acad. Sci. USA 96, 10123–10128.
[8] Schwille, P., Korlach, J. and Webb, W.W. (1999) Cytometry 36, 176–182.
[9] Schwille, P., Haupts, U., Maiti, S. and Webb, W.W. (1999) Biophys. J. 77, 2251–2265.
[10] Terada, S., Kinjo, M. and Hirokawa, N. (2000) Cell 103, 141–155.
[11] Köhler, R.H., Schwille, P., Webb, W.W. and Hanson, M.R. (2000) J. Cell Sci. 113, 3921–3930.
[12] Yoshida, N., Kinjo, M. and Tamura, M. (2001) Biochem. Biophys. Res. Commun. 280, 312–318.
[13] Nomura, Y., Tanaka, H., Poellinger, L., Higashino, F. and Kinjo, M. (2001) Cytometry 44, 1–6.
[14] Nishizuka, Y. (1992) Science 258, 607–614.
[15] Hurley, J.H. and Misra, S. (2000) Annu. Rev. Biophys. Biomol. Struct. 29, 49–79.
[16] Hurley, J.H. and Meyer, T. (2001) Curr. Opin. Cell Biol. 13, 146–152.
[17] Sakai, N., Sasaki, K., Ikegaki, N., Shirai, Y., Ono, Y. and Saito, N. (1997) J. Cell Biol. 139, 1465–1476.
[18] Oancea, E., Teruel, M.N., Quest, A.F.G. and Metyer, T. (1998) J. Cell Biol. 140, 485–498.
[19] Almholt, K., Arkhammar, P.O.G., Thastrup, O. and Tullin, S. (1999) Biochem. J. 337, 211–218.
[20] Mochly-Rosen, D. and Gordon, A.S. (1998) FASEB J. 12, 35–42.
[21] Bacia, K., Majoul, I.V. and Schwille, P. (2002) Biophys. J. 83, 1184–1193.
[22] Palfrey, H.C. and Waseem, A. (1985) J. Biol. Chem. 29, 16021–16029.
[23] Schaefer, M., Albercht, N., Hofmann, T., Gudermann, T. and Schultz, G. (2001) FASEB J. 15, 1634–1636.